Title
Kinematic Signatures of the Projectile Breakup Process at 32.5 MeV/Nucleon

Permalink
https://escholarship.org/uc/item/06w8d0r0

Journal
Physics letters B, 235(3,4)

Authors
Harmon, B.A.
Pouliot, J.
Lopez, J.A.
et al.

Publication Date
1989-10-01

UC-413

LBL-27861
Preprint

Lawrence Berkeley Laboratory
UNIVERSITY OF CALIFORNIA

Submitted to Physics Letters B

Kinematic Signatures of the Projectile Breakup Process at 32.5 MeV/nucleon

B.A. Harmon, J. Pouliot, J.A. López, J. Suro, R. Knop,
Y. Chan, D.E. DiGregorio, and R.G. Stokstad

October 1989

NUCLEAR SCIENCE DIVISION

Prepared for the U.S. Department of Energy under Contract Number DE-AC03-76SF00098.

DISCLAIMER

Kinematic Signatures of the Projectile Breakup Process at 32.5 MeV/nucleon

B. A. Harmon, J. Pouliot, J. A. López, J. Suro,
R. Knop, Y. Chan, D. E. DiGregorio[§], and R. G. Stokstad

Nuclear Science Division, Lawrence Berkeley Laboratory[‡],
1 Cyclotron Rd, Berkeley, CA 94720

Abstract

We have studied projectile breakup reactions in the $^{16}O+^{197}Au$ system at 32.5 MeV/nucleon using an array of 34 phoswich detectors. Correlations among final state fragments were analyzed to determine if the breakup occurs by multifragmentation (simultaneous breakup) or sequential decay. A calculational method developed by López and Randrup was used to predict the kinematic signatures of the two decay modes. A comparison to experiment is presented for three breakup channels consisting of three, four, and five charged particles.

Binary sequential decay and multifragmentation are two extreme modes of decay of a highly excited nucleus. In the former mechanism there is sufficient time between the successive emission of particles to render them independent except for the constraints imposed by conservation laws. In the latter the nucleus breaks up into three or more particles simultaneously and each particle can be influenced by the motion of the other particles through mutual Coulomb repulsion. It is clear that the velocities of the emitted particles will be different in these extremes, even if the initial conditions and the number and type of fragments in the final state are the same. López and Randrup have suggested the possibility of distinguishing between sequential decay and multifragmentation on the basis of these different kinematic signatures, and have developed a numerical model for each extreme [1]. In a recent study, Pouliot *et al.* observed the breakup of ^{16}O projectiles at 32.5 MeV/nucleon into three, four, and five fragments [2]. This letter reports a comparison of the predicted kinematic signatures for sequential decay and multifragmentation with these experimental results. In particular, we consider the kinematical correlations among coincident particles in three breakup channels: B-He-H, He-He-He-He, and He-He-He-H-H, each with total charge equal to that of the projectile.

The experiment was performed at the 88-Inch Cyclotron at the Lawrence Berkeley Laboratory. The products of the reaction ^{16}O+^{197}Au at 32.5 MeV/nucleon were detected by a 34 element array of phoswich detectors [3] that determined the energies, charges, and angles of emission for coincident particles resulting from the breakup of the projectile. The excitation energy of a primary oxygen nucleus was then determined by summing the relative kinetic energy of the emitted particles in the rest frame of the projectile and the separation energy for dissociation into the observed fragments. Reference 2 describes the experiment, the deduction of the excitation energy spectrum for the primary excited nucleus, and the results for the yields of the different exit channels. Here we make use only of the kinematical observables and the deduced excitation spectrum for the oxygen-like primary nucleus; other experimental details can be found in refs. 2 and 3.

Sequential decay implies an equilibrated nucleus that disassembles by the emission of excited fragments in a series of binary, fission-like decays. Each split produces two new equilibrated nuclei that can then undergo further decay if there is sufficient excitation energy. A Monte Carlo treatment of this chain of decays produces a final state composed of nucleons and complex fragments in which the identity and velocity of each of these particles is known. The decay widths for the possible splits are calculated in the context of the Bohr-Wheeler transition state. The calculation proceeds as is discussed in ref. 1, with the exception that the parametrization of the barriers has been changed. Because the nuclei we consider are much lighter, we take the barrier to be the difference between the surface-plus-Coulomb energy of the spherical compound nucleus and that of the fissioned system when the two spherical daughters are in contact. Angular momentum is not included in the present treatment.

If the nucleus considered above decays instead by multifragmentation, and into the same channel reached by sequential decay, the velocities of the fragments are calculated as follows: The final state fragments are first positioned randomly within a sphere whose volume is adjusted to produce the same excitation energy as was available for the sequential decay. The constraining sphere is then removed and the fragments emerge along Coulomb trajectories. This results in a new event that has, by construction, the same fragments and total kinetic energy as the sequential decay, but with kinematic properties inherent to the multifragmentation reaction mechanism. We assume that the emitted particles are cold, i.e., that secondary particle emission does not occur. This is justified in the case of these very light nuclei, whereas in ref. 1 the fragments in the expansion stage contain some excitation energy and are allowed to deexcite by subsequent binary decays.

As in ref. 2, we assume that the decay of the projectile-like source is independent of its prior interaction with the target. The distribution of excitation energy of the primary oxygen for decay into a specific channel is taken directly from the corresponding experimental distribution. The excitation energies are then used as an input to the sequential decay calculation, which determines the distribution of fragments in the final state. The corresponding multifragmentation calculation is performed for the same number of events as the sequential calculation, and with the same fragment distribution. Finally, all events are "filtered" through the experimental apparatus [3] in order to correct for the effects of geometry, energy threshold, angular resolution and multiple hits in a single detector. Free neutrons, which are produced along with charged particles in the calculation, are ignored. This simulates the experimental insensitivity to neutral particles.

The first kinematical correlation we examine is the distribution of relative angles between fragments, taken pairwise, in the rest frame of the primary nucleus. The relative angle is akin to the folding angle for binary fission; however, since there is no special significance of any particular fragment, or fragments, we consider all possible angles. The simplest case is the mass-symmetric channel He-He-He-He. It has the least ambiguity with respect to the isotopic makeup of the final nuclei (all fragments are mostly ^{4}He). The mass symmetry allows one to combine the resulting six pairs of angles to form a single distribution. In Fig. 1, the experimental distribution of relative angles in the He-He-He-He exit channel for 2000 breakup events is shown. The filtered calculations for sequential decay and multifragmentation, normalized by the ratio of calculated events to experimental events (after filtering), are also shown in Fig. 1 for comparison.

The Monte Carlo calculation for sequential decay produces a shape very much like the experimental distribution. These two distributions are also noticeably broader and more skewed than the distribution for multifragmentation. This can be understood on quite general grounds. First, the difference in width of the two distributions arises from the Coulomb repulsion between fragments: in multifragmentation, the trajectories of the four alpha particles are directed away from each other because of mutual Coulomb repulsion. This tends to minimize the differences among the six relative angles. In sequential decay, the particles emitted in different steps are sufficiently removed from each other that mutual Coulomb repulsion is negligible and they therefore have essentially random emission directions (neglecting angular momentum effects). Second, the difference in skewness follows from the presence of intermediate states in sequential decay: a statistical model [2] indicates that the dominant decay routes for the He-He-He-He exit channel are $^{16}O \rightarrow {}^{12}C + {}^4He \rightarrow {}^8Be + {}^4He + {}^4He \rightarrow {}^4He + {}^4He + {}^4He + {}^4He$, and $^{16}O \rightarrow {}^8Be + {}^8Be \rightarrow {}^4He + {}^4He + {}^4He + {}^4He$. The decay of ^{8}Be(g.s.) in these two sequences produces a single small relative angle between two alpha particles, and larger angles for all the remaining pairs. By definition, these intermediate ^{8}Be states are absent in multifragmentation.

The mass-asymmetric exit channels, B-He-H and He-He-He-H-H, may be analyzed in a similar way, except that we do not combine all angle combinations together in one distribution. Instead, the relative angle combinations are grouped according to particle type, yielding three distributions each for B-He-H and He-He-He-H-H. We find that the second moment, or width of the distribution, is useful for distinguishing between the two decay mechanisms when the multiplicity is not too large. In Fig. 2, the standard deviations (σ) of the six relative angle distributions for the two exit channels are shown. As was the case with the mass-symmetric channel, sequential emission predicts a broader relative angle distribution than multifragmentation. Again, the sequential mechanism is in better agreement with the data. The origins of the remaining discrepancies in the moments for B-He and He-He could conceivably lie with either the simplicity of the schematic model (see ref. 1), or with basic assumptions made in the analysis of the data (see ref. 2). We note (see Fig. 2) that the magnitude of the discrepancy for the width of the B-He distribution between theory (sequential decay) and experiment is about 50%, while that for He-He is only about 11%. The overall uncertainty on the standard deviations plotted in Fig. 2 are approximately ±2 degrees, depending on the number of events in the sample. Filtering has only a small effect on these second moments: the values for the filtered and unfiltered results differ by no more than three or four degrees for the three decay channels.

Another kinematic method, useful in analyzing the general character of a breakup reaction, is to identify macroscopic observables that describe the entire fragmenting system. From the momentum vectors of all the emitted fragments, one can construct the kinetic flow tensor and its eigenvectors [4]. The eigenvectors define an ellipsoid in momentum space whose shape can be expressed in terms of *sphericity* and *coplanarity* shape parameters (see ref. 1). Here we examine the shape of the momentum ellipsoid for an ensemble of breakup events. Sphericity-coplanarity plots of the experimental results, and those of the two decay mechanisms, are shown for the exit channel He-He-He-H-H in Fig. 3. Each scatter plot represents a sampling of 500 events. The calculated results consist of a mixture of yields from exit channels of different hydrogen isotopes, ^{1}H-^{1}H, ^{2}H-^{1}H, and ^{2}H-^{2}H. Contributions from He isotopes other than ^{4}He are negligible. The parameter space is bounded by lines connecting vertices at (0,0), $(\frac{3}{4},\frac{\sqrt{3}}{4})$ and (1,0), which correspond, respectively, to the ellipsoidal shapes of a rod, disk, and sphere, as shown in the top frame of the figure. Multifragmentation tends to produce a more uniform distribution of fragment momenta, whereas a sequential decay yields a more elongated distribution. A comparison of the concentrations of events in the lower left corner of each plot reveals a strong "back to back" or rod-like component in the calculated sequential distribution and in the experiment, but not in the prediction for multifragmentation.

A quantitative comparison of the two models with the experimental result is given in Table I for all three exit channels. The average values, before and after filtering, are listed for each channel. The importance of including the effects of filtering on the theoretical predictions is evident. The larger effect of filtering on the average sphericity and coplanarity, as compared to the moments of the relative angle distributions, is related to the global nature of the sphericity-coplanarity analysis method, which involves both the direction and magnitude of all the fragment velocity vectors.

The agreement between the filtered sequential decay calculation and the experiment is generally excellent. The exception is the B-He-H exit channel, which has an average sphericity and coplanarity falling between the predictions for multifragmentation and sequential decay. Since this comparison might suggest a component of multifragmentation, possibly present at higher projectile excitations, a study was made of the excitation energy dependence of the experimental results for both B-He-H and He-He-He-He. The introduction of cuts on the excitation energy of the primary oxygen nucleus, in 10 MeV bins from threshold up to approximately 50 MeV, did not produce a significant dependence on energy in the sphericity-coplanarity or relative angle distributions. Given this and the general agreement with the sequential decay calculations, we conclude that the present experiment does not provide any evidence for multifragmentation of the projectile.

[§] Permanent Address: Departamento de Fisica - TANDAR, Comisión Nacional de Energia Atómica, 1429 Buenos Aires, Argentina and CONICET.

[‡] Work supported under contracts DE-AC03-76SF00098 and DE-AM03-76SF000326 with the U.S. Department of Energy.

References

[1] J. A. López and J. Randrup, Nucl. Phys. **A491**, (1989) 477.

[2] J. Pouliot *et al.*, Phys. Letts. **223 B**, (1989) 16.

[3] J. Pouliot *et al.*, Nucl. Instr. and Meth. **A270**, (1988) 69.

[4] M. Gyulassy, K. A. Frankel and H. Stocker, Phys. Lett. **110B**, (1982) 185.

Table I

Average Values of Sphericity and Coplanarity

	Channel					
	B-He-H		He-He-He-He		He-He-He-H-H	
	SPH	COP	SPH	COP	SPH	COP
MF	.138±.002 (.154)*	.068±.001 (.075)	.291±.003 (.302)	.140±.001 (.142)	.231±.004 (.267)	.094±.002 (.100)
SEQ	.070±.002 (.094)	.033±.001 (.042)	.190±.003 (.152)	.097±.002 (.079)	.163±.005 (.148)	.075±.003 (.071)
DATA	.122±.003	.055±.001	.191±.004	.101±.002	.168±.006	.080±.003

*( ) represents unfiltered result of calculation.

Figure Captions

1. Experimental distribution of relative angles for the He-He-He-He exit channel (histogram) and the corresponding predictions for sequential decay and multifragmentation (solid and dashed curves).

2. A comparison of the standard deviations (σ) for the experimental relative angle distribution with the predicted results for sequential decay and multifragmentation in the B-He-H and He-He-He-H-H exit channels. The experimental results are joined by solid lines and the calculations by dashed lines for clarity.

3. Experimental coplanarity-sphericity distribution for the He-He-He-H-H exit channel (top) and the predicted distributions for sequential decay (center) and multifragmentation (bottom). Each plot is a sampling of 500 breakup events.

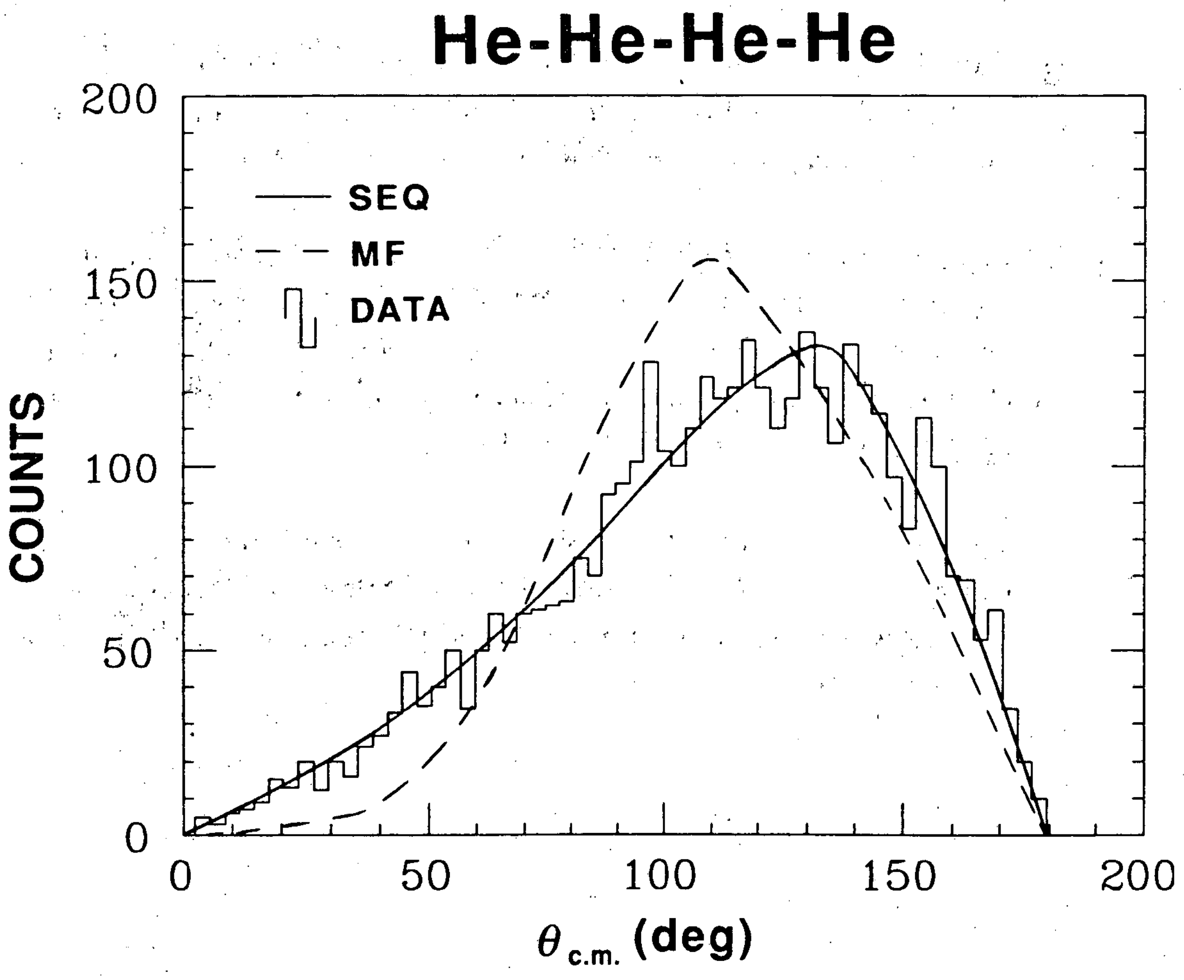

XBL 899-3291

Fig. 1

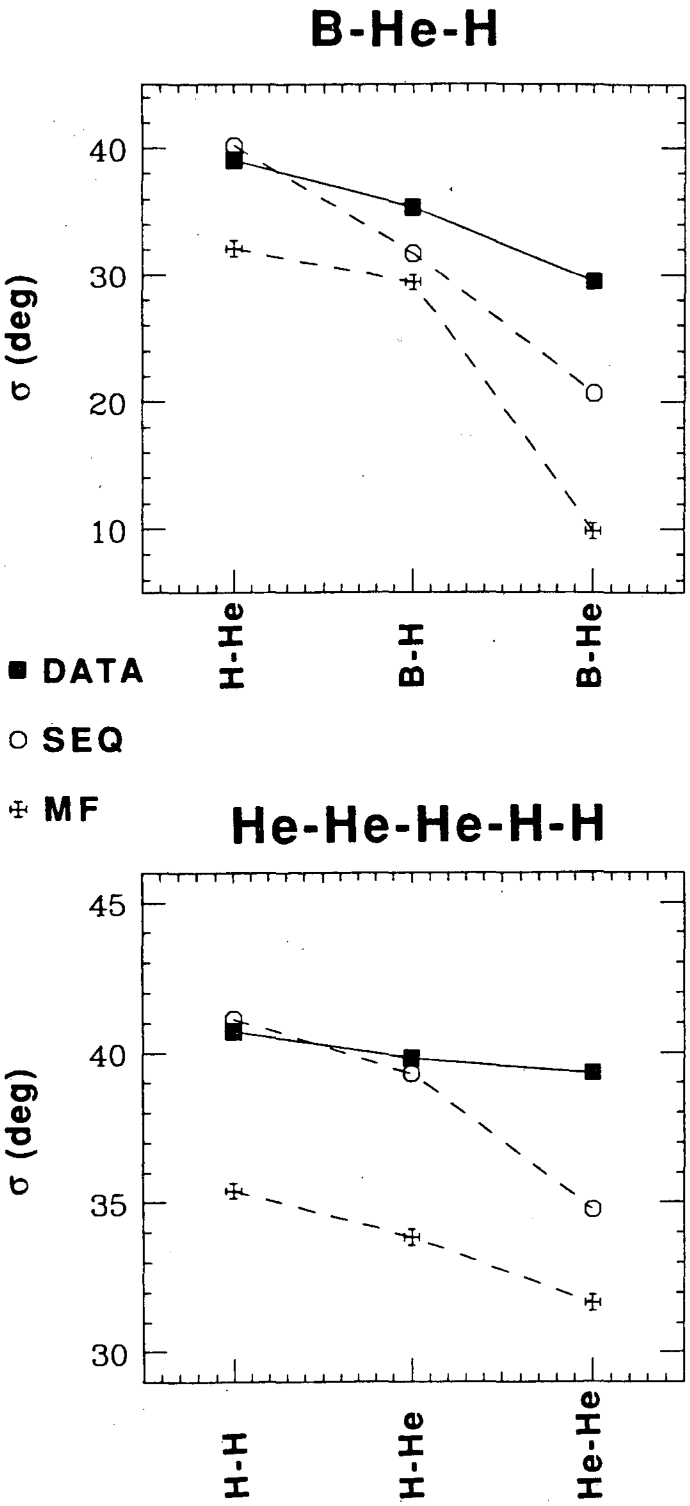

XBL 899-3290

Fig. 2

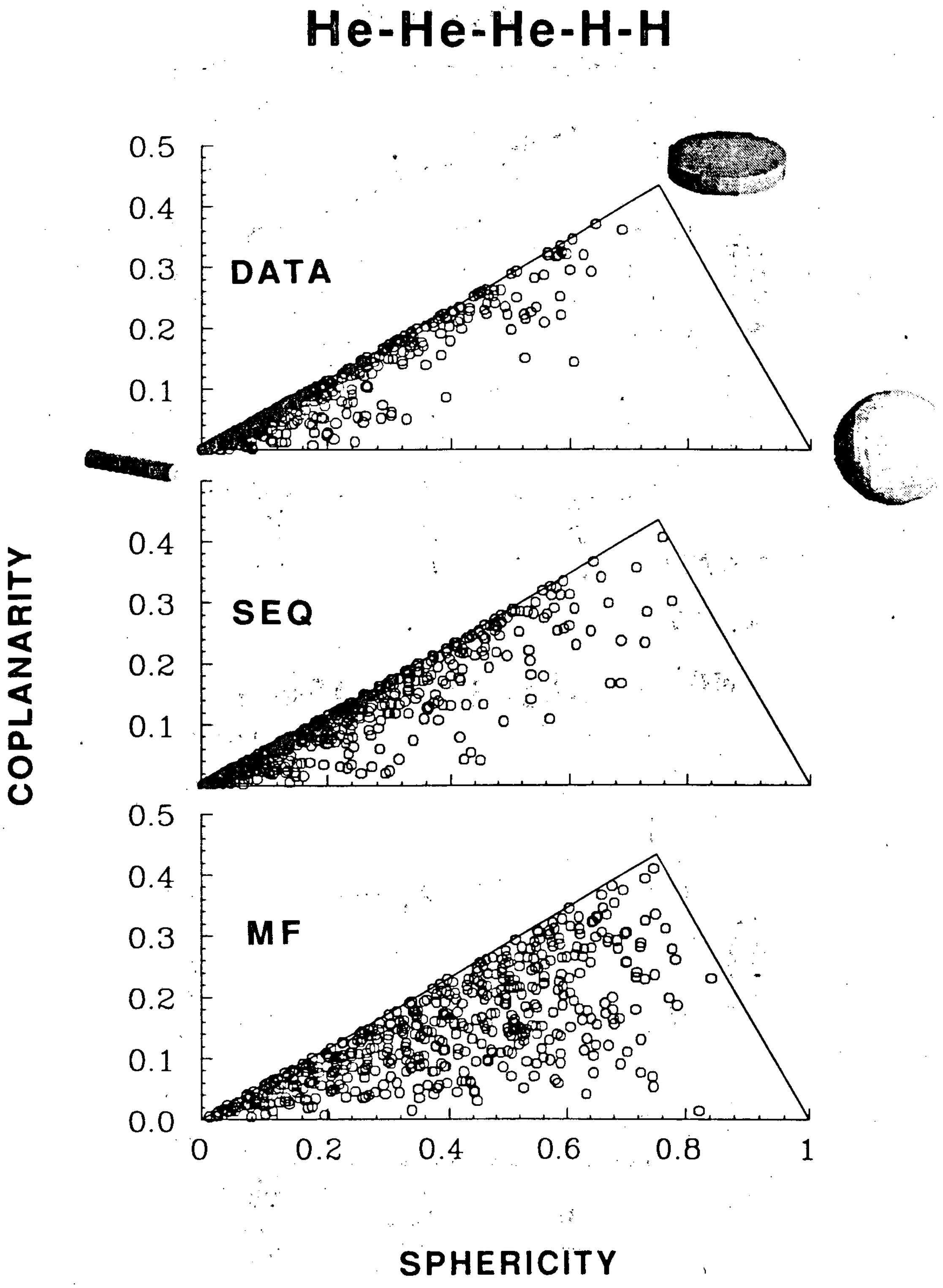

XBL 899-3292

Fig. 3